Chapter 8
The Newmark Method and a Moving Inertial Load

The Newmark method (see Section 5.5) is considered here as a representative example of a wide family of time integration methods. It is attractive since most of computational procedures in structural dynamics are based on this numerical scheme.

8.1 The Newmark Method in Moving Mass Problems

We must emphasize here that the matrices derived contribute only the point mass effects. They must be simply added to the classical matrices elaborated for a structure, i.e., for a string or a beam. The full discrete motion equation is

$$(\mathbf{M}+\mathbf{M}_m)\ddot{\mathbf{w}}^{i+1} + (\mathbf{C}+\mathbf{C}_m)\dot{\mathbf{w}}^{i+1} + (\mathbf{K}+\mathbf{K}_m)\mathbf{w}^{i+1} = \mathbf{F}^{i+1} + \mathbf{e}_m^i \,, \tag{8.1}$$

where $\mathbf{M}$ is the inertia matrix of the structure, $\mathbf{M}_m$ is the moving mass matrix, added only to the inertia matrix of the element on which it travels. The same occurs in the case of the damping matrix of the structure $\mathbf{C}$ and the point mass $\mathbf{C}_m$, and in the case of the stiffness matrix of the structure $\mathbf{K}$ and the point mass $\mathbf{K}_m$. The vector $\mathbf{F}^{i+1}$ is the vector of external forces established at time t_{i+1} and $\mathbf{e}_m^i$ is the right-hand side vector resulting from the the mass inertia term, established at the beginning of the time interval $[t_i, t_{i+1}]$. We will concentrate our attention on the mass influence only, thus we will derive the matrices $\mathbf{M}_m$, $\mathbf{C}_m$, $\mathbf{K}_m$, and $\mathbf{e}_m^i$ in the following equation

$$\mathbf{M}_m\ddot{\mathbf{w}}^{i+1} + \mathbf{C}_m\dot{\mathbf{w}}^{i+1} + \mathbf{K}_m\mathbf{w}^{i+1} = \mathbf{e}_m^i \,, \tag{8.2}$$

where the vector of nodal displacements in the case of beams is $\mathbf{w} = [w_1, \psi_1, w_2, \psi_2]$, and that in the case of a string is $\mathbf{w} = [w_1, w_2]$.

The matrices of the finite element that carry the inertial particle are composed, as a sum, of two sets: the matrices describing the element of the structure and the matrices that incorporate the mass influence. Since the elemental matrices are well known, below we will consider only the influence of the mass.

The solution of this problem concerns a mass particle moving on a general finite element. This can be applied to all types of structures: strings, beams, plates, shells,

C.I. Bajer and B. Dyniewicz: Numerical Analysis of Vibrations of Structures, LNACM 65, pp. 223–240.
springerlink.com

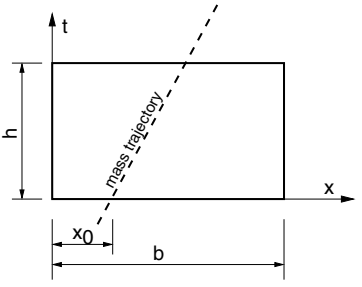

Fig. 8.1 The mass trajectory in space and time.

etc. Below we will derive the resulting matrices which will then be applied and tested with a string, an Euler beam, and a Timoshenko beam.

Let us consider a finite element of length b of the edge of the mass trajectory. The mass particle m passes through the finite element with velocity v in the time interval h, starting at the point $x = x_0$ (Figure 8.1). The equation of virtual work which describes the motion of the inertial particle is

$$\Pi_m = \int_0^b w^*(x)\,\delta(x - x_0 - \mathsf{v}t)\,m\,\frac{\mathrm{d}^2 w(\mathsf{v}t,t)}{\mathrm{d}t^2}\mathrm{d}x\,, \tag{8.3}$$

where the position of the moving point can be described by the function $x = \mathsf{v}t$. The virtual displacement function w^* is given by

$$w^*(x) = \left[1 - \frac{x}{b}, \frac{x}{b}\right]\mathbf{w}\,. \tag{8.4}$$

We take first-order polynomials as the shape functions describing the interpolation of the displacements:

$$w(x,t) = \left(1 - \frac{x}{b}\right)w_1(t) + \frac{x}{b}w_2(t)\,. \tag{8.5}$$

Here, $w_1(t)$ and $w_2(t)$ are the nodal displacements in time. This is a natural assumption since the finite element edge is straight in cases of simple shape functions describing linear displacement distributions in the element. In such a case, the third term of (7.1) reduces to zero. That is why we must write the Renaudot formula (7.1) at constant speed in a different form:

$$\frac{\mathrm{d}^2 w(\mathsf{v}t,t)}{\mathrm{d}t^2} = \left.\frac{\partial^2 w(x,t)}{\partial t^2}\right|_{x=\mathsf{v}t} + \mathsf{v}\left.\frac{\partial^2 w(x,t)}{\partial x \partial t}\right|_{x=\mathsf{v}t} + \mathsf{v}\frac{\mathrm{d}}{\mathrm{d}t}\left[\left.\frac{\partial w(x,t)}{\partial x}\right|_{x=\mathsf{v}t}\right]. \tag{8.6}$$

The third term of (8.6) is developed in its Taylor series in terms of the time increment $\Delta t = h$

$$\left[\left.\frac{\partial w(x,t)}{\partial x}\right|_{x=\mathsf{v}t}\right]^{t+h} = \left[\left.\frac{\partial w(x,t)}{\partial x}\right|_{x=\mathsf{v}t}\right]^{t} + \\ + \left\{\frac{\mathrm{d}}{\mathrm{d}t}\left[\left.\frac{\partial w(x,t)}{\partial x}\right|_{x=\mathsf{v}t}\right]\right\}^{t}(1-\gamma)h + \left\{\frac{\mathrm{d}}{\mathrm{d}t}\left[\left.\frac{\partial w(x,t)}{\partial x}\right|_{x=\mathsf{v}t}\right]\right\}^{t+h}\gamma h. \tag{8.7}$$

The upper indices indicate the time at which the respective terms are defined. We assume the backward difference formula ($\gamma = 1$). In this case we have

$$\left\{\frac{\mathrm{d}}{\mathrm{d}t}\left[\left.\frac{\partial w(x,t)}{\partial x}\right|_{x=\mathsf{v}t}\right]\right\}^{t+h} = \frac{1}{h}\left[\left.\frac{\partial w(x,t)}{\partial x}\right|_{x=\mathsf{v}t}\right]^{t+h} - \frac{1}{h}\left[\left.\frac{\partial w(x,t)}{\partial x}\right|_{x=\mathsf{v}t}\right]^{t}. \tag{8.8}$$

Using (8.5) and (8.8), the equation (8.6) is given by the difference formula

$$\frac{\mathrm{d}^2 w}{\mathrm{d}t^2} = \left(1 - \frac{x_0 + \mathsf{v}t}{b}\right)\ddot{w}_1^{i+1} + \frac{x_0 + \mathsf{v}t}{b}\ddot{w}_2^{i+1} - \frac{\mathsf{v}}{b}\dot{w}_1^{i+1} + \frac{\mathsf{v}}{b}\dot{w}_2^{i+1} - \\ - \frac{\mathsf{v}}{bh}w_1^{i+1} + \frac{\mathsf{v}}{bh}w_2^{i+1} + \frac{\mathsf{v}}{bh}w_1^{i} - \frac{\mathsf{v}}{bh}w_2^{i}\,. \tag{8.9}$$

The upper index denotes the time layer. The energy (8.3), with respect to (8.4) and (8.9) can be written in quadratic form, which, after a classical minimization, results in the matrix equation (8.2), where

$$\mathbf{M}_m = m\begin{bmatrix} (1-\kappa)^2 & 0 & \kappa(1-\kappa) & 0 \\ 0 & 0 & 0 & 0 \\ \kappa(1-\kappa) & 0 & \kappa^2 & 0 \\ 0 & 0 & 0 & 0 \end{bmatrix}, \tag{8.10}$$

$$\mathbf{C}_m = \frac{m\mathsf{v}}{b}\begin{bmatrix} -(1-\kappa) & 0 & 1-\kappa & 0 \\ 0 & 0 & 0 & 0 \\ -\kappa & 0 & \kappa & 0 \\ 0 & 0 & 0 & 0 \end{bmatrix}, \tag{8.11}$$

$$\mathbf{K}_m = \frac{m\mathsf{v}}{bh}\begin{bmatrix} -(1-\kappa) & 0 & 1-\kappa & 0 \\ 0 & 0 & 0 & 0 \\ -\kappa & 0 & \kappa & 0 \\ 0 & 0 & 0 & 0 \end{bmatrix}, \tag{8.12}$$

and

$$\mathbf{e}_m = \frac{m\mathsf{v}}{bh}\begin{bmatrix}(1-\kappa)(w_2-w_1)\\ 0\\ \kappa(w_2-w_1)\\ 0\end{bmatrix}, \tag{8.13}$$

with coefficient $\kappa = (x_0 + \mathsf{v}h)/b$, $0 < \kappa \leq 1$. κ is a parameter which defines the position of the mass in the element at the beginning of the time increment.

This determines the position of the mass at time $t = h$, related to the finite element length b. The different terms describe the transverse inertia force related to the vertical acceleration, the Coriolis force, and the centrifugal force. The matrix factors $\mathbf{M}_m$, $\mathbf{C}_m$, and $\mathbf{K}_m$ can be called the mass, the damping, and the stiffness matrices. The last term $\mathbf{e}_m$ describes the nodal forces at the beginning of the time interval $[t_i, t_i + \Delta t]$. We must emphasize here that the matrices (8.10)–(8.12) and the vector (8.13) contribute only the moving inertial particle effect. The matrices of the mass influence in a finite element of a structure must be added to the global system of equations. We notice that the matrices (8.10)–(8.12) differ from the matrices that result from the solution for the case of direct differentiation of (7.1).

8.2 The Newmark Method in the Vibrations of String

The finite element of a string that carries an inertial particle was tested with the use of the Newmark method. In each time-step, the global matrices $\mathbf{M}$, $\mathbf{C}$, and $\mathbf{K}$ must be computed since the contributions of (8.10)–(8.12) vary. The string being tested has dimensionless length $l = 1$, tensile force $N = 1$, cross-sectional area $A = 1$, and mass density $\rho = 1$. The travelling mass $m = 1$ was accompanied by the force $P = -1$ (Figure 8.2). Figure 8.3 depicts the mass trajectory at various speeds v. This diagram can be compared with the semi-analytical results depicted in Figure 3.3. We note good coincidence for a whole range of speeds. Moreover, the discontinuity at the final support is exhibited in the numerical results. This discontinuity was reported in [48] and was also obtained by the space–time finite element method [25]. The mid-span deflections are depicted in Figure 8.4. The method can also be applied to over-critical speed (Figures 8.5 and 8.6).

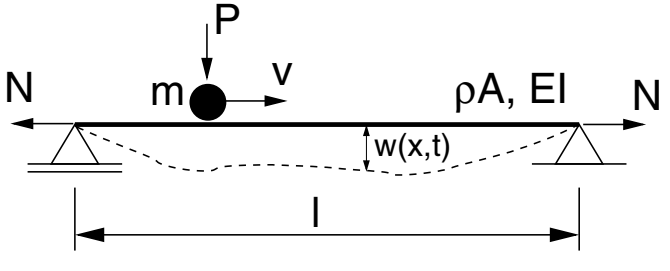

Fig. 8.2 The scheme of the tested system.

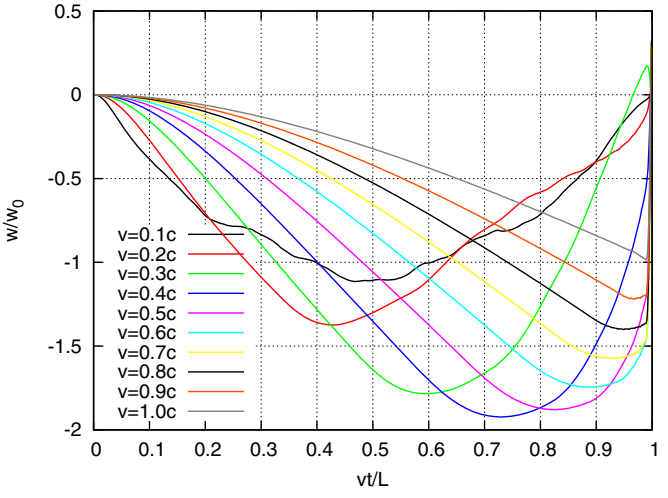

Fig. 8.3 The mass trajectory at velocities 0.1–1.0 times the wave speed c, computed numerically by the Newmark method.

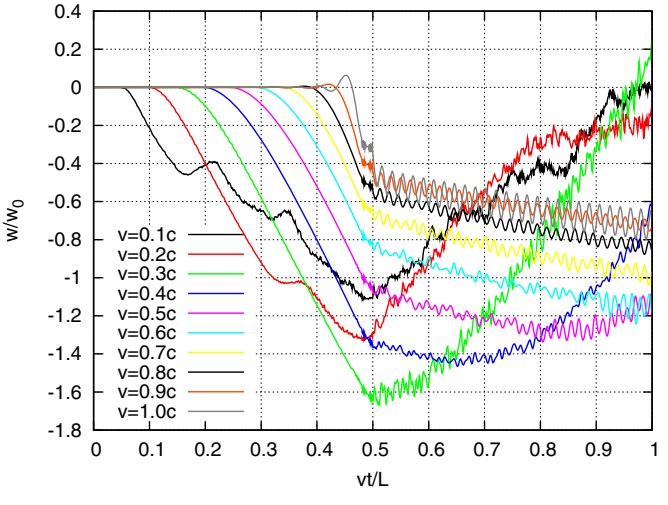

Fig. 8.4 The displacement of the middle of the span at velocities 0.1–1.0 times the wave speed c.

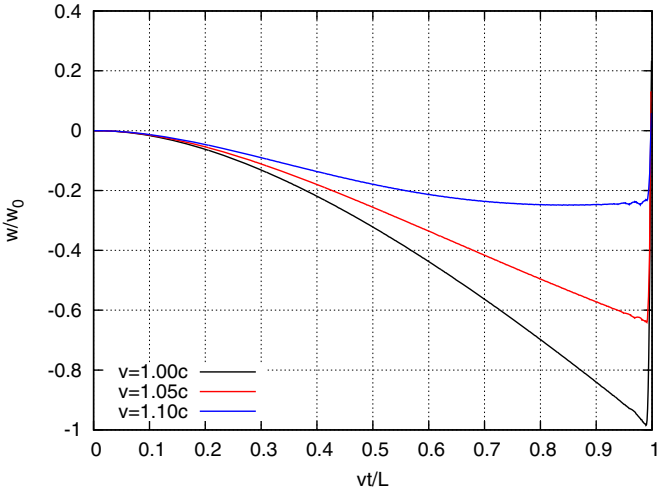

Fig. 8.5 The mass trajectory at velocities 1.0–1.1 times the wave speed c, computed numerically by the Newmark method.

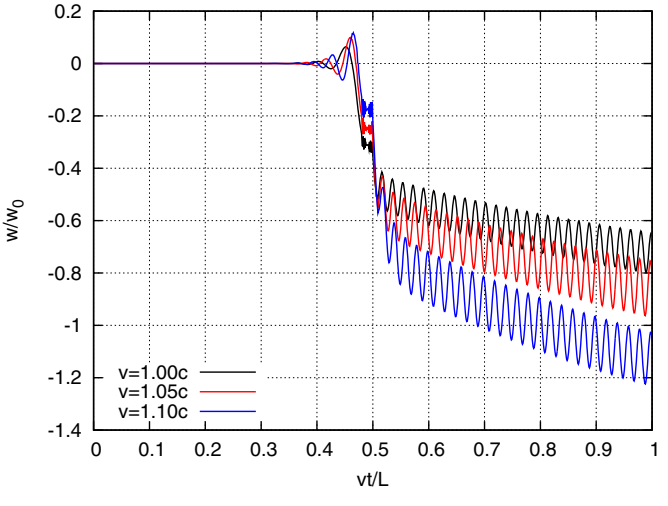

Fig. 8.6 The displacement of the middle of the span at velocities 1.0–1.1 times the wave speed c.

8.3 The Newmark Method in Vibrations of the Bernoulli–Euler Beam

The solution procedure is relatively simple in the case of the Bernoulli–Euler beam with third order shape functions. The characteristic matrices can be easily derived (8.14)–(8.16). We use them in verification of various results from the literature:

$$\mathbf{M}_m = m \begin{bmatrix} (2\kappa^3-3\kappa^2+1)^2 & b\kappa(\kappa^2-2\kappa+1)(2\kappa^3-3\kappa^2+1) \\ b\kappa(\kappa^2-2\kappa+1)(2\kappa^3-3\kappa^2+1) & b^2\kappa^2(\kappa^2-2\kappa+1)^2 \\ \kappa^2(3-2\kappa)(2\kappa^3-3\kappa^2+1) & b\kappa^3(3-2\kappa)(\kappa^2-2\kappa+1) \\ b\kappa^2(\kappa-1)(2\kappa^3-3\kappa^2+1) & b^2\kappa^3(\kappa-1)(\kappa^2-2\kappa+1) \end{bmatrix}$$

$$\begin{matrix} \kappa^2(3-2\kappa)(2\kappa^3-3\kappa^2+1) & b\kappa^2(\kappa-1)(2\kappa^3-3\kappa^2+1) \\ b\kappa^3(3-2\kappa)(\kappa^2-2\kappa+1) & b^2\kappa^3(\kappa-1)(\kappa^2-2\kappa+1) \\ \kappa^4(2\kappa-3)^2 & b\kappa^4(1-\kappa)(2\kappa-3) \\ b\kappa^4(1-\kappa)(2\kappa-3) & b^2\kappa^4(\kappa-1)^2 \end{matrix} \Bigg] \quad (8.14)$$

$$\mathbf{C}_m = 2m\mathsf{v} \begin{bmatrix} 6\kappa(\kappa-1)(2\kappa^3-3\kappa^2+1)/b & (3\kappa^2-4\kappa+1)(2\kappa^3-3\kappa^2+1) \\ 6\kappa^2(\kappa-1)(\kappa^2-2\kappa+1) & b\kappa(\kappa^2-2\kappa+1)(3\kappa^2-4\kappa+1) \\ 6\kappa^3(1-\kappa)(2\kappa-3)/b & \kappa^2(3-2\kappa)(3\kappa^2-4\kappa+1) \\ 6\kappa^3(\kappa-1)^2 & b\kappa^2(\kappa-1)(3\kappa^2-4\kappa+1) \end{bmatrix}$$

$$\begin{matrix} 6\kappa(1-\kappa)(2\kappa^3-3\kappa^2+1)/b & \kappa(3\kappa-2)(2\kappa^3-3\kappa^2+1) \\ 6\kappa^2(1-\kappa)(\kappa^2-2\kappa+1) & b\kappa^2(\kappa^2-2\kappa+1)(3\kappa-2) \\ 6\kappa^3(\kappa-1)(2\kappa-3)/b & \kappa^3(3-2\kappa)(3\kappa-2) \\ -6\kappa^3(\kappa-1)^2 & b\kappa^3(\kappa-1)(3\kappa-2) \end{matrix} \Bigg] , \quad (8.15)$$

$$\mathbf{K}_m = m\mathsf{v}^2 \begin{bmatrix} 6(2\kappa-1)(2\kappa^3-3\kappa^2+1)/b^2 & 2(3\kappa-2)(2\kappa^3-3\kappa^2+1)/b \\ 6\kappa(\kappa^2-2\kappa+1)(2\kappa-1)/b & 2\kappa(\kappa^2-2\kappa+1)(3\kappa-2) \\ 6\kappa^2(1-2\kappa)(2\kappa-3)/b^2 & 2\kappa^2(3-2\kappa)(3\kappa-2)/b \\ 6\kappa^2(\kappa-1)(2\kappa-1)/b & 2\kappa^2(\kappa-1)(3\kappa-2) \end{bmatrix}$$

$$\begin{matrix} 6(1-2\kappa)(2\kappa^3-3\kappa^2+1)/b^2 & 2(3\kappa-1)(2\kappa^3-3\kappa^2+1)/b \\ 6\kappa(1-2\kappa)(\kappa^2-2\kappa+1)/b & 2\kappa(\kappa^2-2\kappa+1)(3\kappa-1) \\ 6\kappa^2(2\kappa-1)(2\kappa-3)/b^2 & 2\kappa^2(3-2\kappa)(3\kappa-1)/b \\ 6\kappa^2(1-\kappa)(2\kappa-1)/b & 2\kappa^2(\kappa-1)(3\kappa-1) \end{matrix} \Bigg] , \quad (8.16)$$

where the parameter $\kappa = (x_0 + \mathsf{v}h)/b$, x_0 is the initial position of the mass moving with speed v on the spatial element of length b in the time interval h.

8.4 The Newmark Method in Vibrations of a Timoshenko Beam

The study of wave phenomena is possible by using a more complex model of the Timoshenko beam in which the vibration equation takes into account the influence of lateral forces and rotatory inertia on the deflection line of the beam. The angle formed by the axis of the deformed beam is composed of the pure bending angle and the angle corresponding to the deformation of the pure shear. Independent interpolation of the displacements and rotation angles of the Timoshenko beam causes serious problems. Linear interpolation (8.5) of the nodal shape features renders impossible the determination of the centrifugal acceleration of the moving mass particle. Direct discretization of the terms (7.1), placed in the governing differential equation of motion, results in the following matrices:

$$\mathbf{M}_m = m \begin{bmatrix} (1-\kappa)^2 & 0 & \kappa(1-\kappa) & 0 \\ 0 & 0 & 0 & 0 \\ \kappa(1-\kappa) & 0 & \kappa^2 & 0 \\ 0 & 0 & 0 & 0 \end{bmatrix}, \tag{8.17}$$

$$\mathbf{C}_m = \frac{2m\mathrm{v}}{b} \begin{bmatrix} -(1-\kappa) & 0 & 1-\kappa & 0 \\ 0 & 0 & 0 & 0 \\ -\kappa & 0 & \kappa & 0 \\ 0 & 0 & 0 & 0 \end{bmatrix}, \tag{8.18}$$

$$\mathbf{K}_m = \mathbf{0}\,, \tag{8.19}$$

with the coefficient

$$\kappa = \frac{x_0 + \mathrm{v}h}{b}\,,\ 0 < \kappa \leq 1. \tag{8.20}$$

We can apply these to a test problem and then compare the results with those obtained by semi-analytical methods. Unfortunately, the comparison is extremely unsatisfactory, especially if applied to strictly hyperbolic problems (see for example [48]). We must emphasize here that the matrices (8.10)–(8.12) and the vector (8.13) contribute only the moving inertial particle effect. The matrices of a mass influence in a finite element of the Timoshenko beam must be added to the global system of equations. Note that the matrices (8.17)–(8.19) differ from the matrices (8.10)–(8.13). The matrix $\mathbf{M}$ is the only matrix that is the same.

8.5 Numerical Results

There are few publications in which an inertial load moving on a Timoshenko beam are directly considered numerically. One can see that papers published in the literature describe methods which result in wrong responses. We can show results taken

from the literature compared with semi-analytical computations. A comparison with the paper [148] is given in Figure 4.15. In the example, a very low relative velocity was assumed: $v/c_1 = 0.002$ and $v/c_2 = 0.001$ (shear wave and bending wave, respectively).

We will compare our diagrams with those of Lee [86]. Therefore, the data in the example is as follows: length $l = 1$ m, Young modulus $E = 207$ GPa, shear modulus $G = 77.6$ GPa, mass density $\rho = 7700$ kg/m^3. The velocity $v = a\pi/l \cdot \sqrt{EI/\rho/A}$

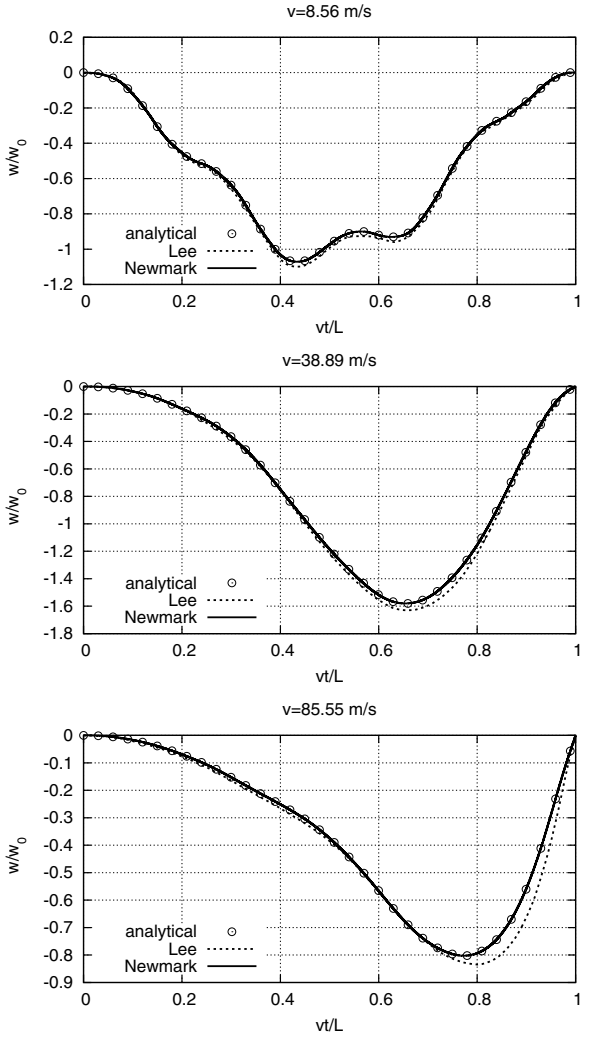

Fig. 8.7 Normalized deflections under a moving mass particle for $\beta = 0.03$: (a) $a = 0.11$, (b) $a = 0.5$ and (c) $a = 1.1$.

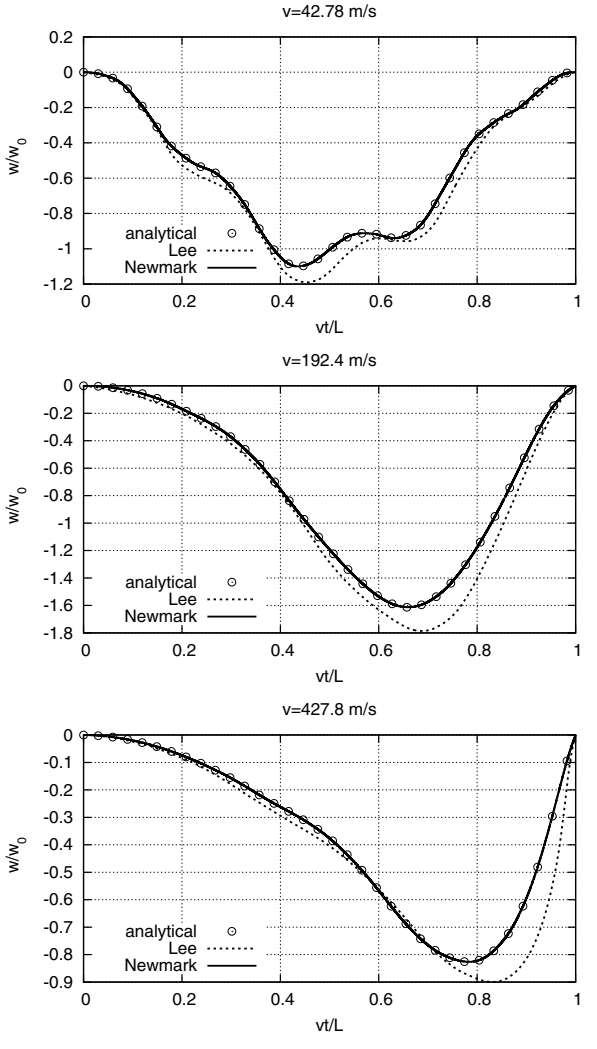

Fig. 8.8 Normalized deflections under a moving mass particle for $\beta = 0.15$: (a) $a = 0.11$, (b) $a = 0.5$ and (c) $a = 1.1$.

was determined by the parameter a. Another parameter β determines the cross sectional area $A = \beta^2 l^2/\pi$ and cross sectional inertia moment $I = \beta^4 l^4/4/\pi^3$. The moving mass m took values of 0.441 kg and 11.03 kg. Figure 8.7 exhibits the normalized deflection under the moving mass for $\beta = 0.03$ and $a = 0.11$, 0.5, and 1.1. This corresponds to a mass moving at 8.56, 38.39, 85.55 m/s on a relatively elastic beam. Figure 8.8 relates to a more rigid beam and velocities of $\mathrm{v} = 42.78$, 194.4, and 427.7 m/s. Lee solved the problem semi-analytically. A fourth order differential equation was solved by the Fourier transform and finally integrated by the

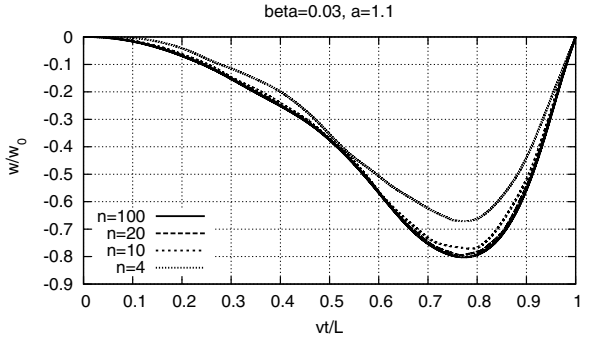

Fig. 8.9 Accuracy of the Newmark method depending on the number of finite elements.

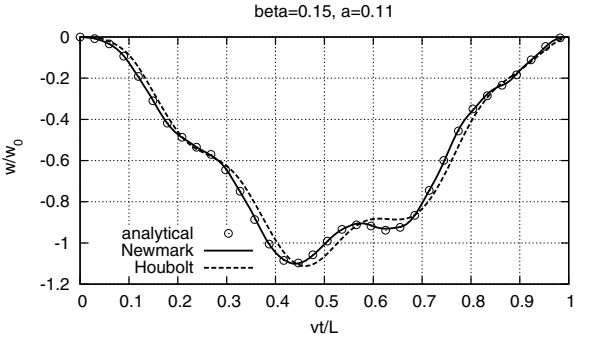

Fig. 8.10 Comparison of the Newmark and Houbolt methods in the case of a large time step.

Runge–Kutta method. In our test, we compare the results by Lee with our semi-analytically [49] obtained curves together with our Newmark time integration procedure applied to the finite element model of the Timoshenko beam. We notice a perfect coincidence of both solutions and quite good coincidence with Lee's results.

Figure 8.9 shows the accuracy, which increases with the number of elements in the structure. Ten to twenty elements is sufficient in our example.

Another comparison was carried out between the Newmark and Houbolt methods. Both methods are sufficiently accurate. However, the curve for the Newmark method perfectly coincides with our semi-analytical results (Figure 8.10).

8.6 Accelerating Mass—Numerical Approach

8.6.1 Mathematical Model

Let us consider the differential equations of structures containing a concentrated mass. We will focus our attention on the term which describes the forces induced by

a moving inertial particle. In the case of a string, we can write the equation in the form

$$-N\frac{\partial^2 w(x,t)}{\partial x^2}+\rho A\frac{\partial^2 w(x,t)}{\partial t^2}=\delta(x-f(t))P-\delta(x-f(t))m\frac{\mathrm{d}^2 w(f(t),t)}{\mathrm{d}t^2}\ . \quad (8.21)$$

Here, $w(x,t)$ is the vertical deflection of the mid-line, m is the moving mass, $f(t)$ is the function giving the distance travelled by the mass, N is the tension of the string, ρA is the mass density per unit length, P is the external point force, and it usually contributes a gravitation force mg.

We impose initial conditions $w(x,0)=0,\ \partial w(x,t)/\partial t\,|_{t=0}\ =\ 0$ and boundary conditions $w(0,t)=0,\ w(l,t)=0$.

The Bernoulli–Euler beam is described by the equation

$$EI\frac{\partial^4 w(x,t)}{\partial x^4}+\rho A\frac{\partial^2 w(x,t)}{\partial t^2}=\delta(x-f(t))P-\delta(x-f(t))m\frac{\mathrm{d}^2 w(f(t),t)}{\mathrm{d}t^2}\ , \quad (8.22)$$

with initial conditions $w(x,0)=0,\ \partial w(x,t)/\partial t\,|_{t=0}\ =\ 0$ and boundary conditions $w(0,t)=0,\ w(l,t)=0, \partial^2 w(0,t)/\partial x^2=0, \partial^2 w(l,t)/\partial x^2=0$, and the Timoshenko beam is

$$\begin{aligned}\rho A\frac{\partial^2 w(x,t)}{\partial t^2}-\frac{GA}{k}\left(\frac{\partial^2 w(x,t)}{\partial x^2}-\frac{\partial\psi(x,t)}{\partial x}\right)=\\ =\delta(x-f(t))P-\delta(x-f(t))m\frac{\mathrm{d}^2 w(f(t),t)}{\mathrm{d}t^2},\end{aligned} \quad (8.23)$$

$$\rho I\frac{\partial^2\psi(x,t)}{\partial t^2}-EI\frac{\partial 2\psi(x,t)}{\partial x^2}-\frac{GA}{k}\left(\frac{\partial w(x,t)}{\partial x}-\psi(x,t)\right)=0\ ,$$

with the same boundary and initial conditions as for the Bernoulli–Euler beam. Here, EI is the bending stiffness, GA/k is the shear stiffness, ρI is the rotatory inertia of the cross section of the beam, and ψ is the angle of rotation of the cross section.

In each type of problem we have the identical inertial term $\delta(x-f(t))m\cdot \mathrm{d}^2 w(f(t),t)/\mathrm{d}t^2$. Below we will consider only this term, since the remaining parts of the equations are treated in the classical way by the finite element method.

Let us follow the direct derivation commonly carried on in the literature. The acceleration of a mass particle moving at a varying speed v in the space–time domain is described by the Renaudot formula:

$$\begin{aligned}\frac{\mathrm{d}^2 w(f(t),t)}{\mathrm{d}t^2}=\left.\frac{\partial^2 w(x,t)}{\partial t^2}\right|_{x=f(t)}+2\mathsf{v}\left.\frac{\partial^2 w(x,t)}{\partial x\partial t}\right|_{x=f(t)}+\mathsf{v}^2\left.\frac{\partial^2 w(x,t)}{\partial x^2}\right|_{x=f(t)}+\\ +\dot{\mathsf{v}}\left.\frac{\partial w(x,t)}{\partial x}\right|_{x=f(t)},\end{aligned} \quad (8.24)$$

where $f(t)$ describes the position of the load. The above formula simply represents the chain rule of differentiation. The corresponding parts of the equation describe the lateral acceleration, the Coriolis acceleration, the centrifugal acceleration, and the acceleration associated with the change of particle velocity. These names are generally not adequate in the case of all structures. Let us compare two different problems: the vibrations of a string and the longitudinal vibrations of a bar. In both cases, we have the identical governing equation. However, in the case of longitudinal displacements we can not call the forces described by the terms of the equation either centrifugal or Coriolis.

8.6.2 The Finite Element Carrying the Moving Mass Particle

Let us consider a finite element of length b of the edge of the mass trajectory. The mass particle m passes through the finite element with a varying velocity v in the time interval h, starting at the point $x = x_0$ (Figure 8.1). The equation of virtual work which describes the motion of the inertial particle can be written in the following form

$$\Pi_m = \int_0^b w^*(x)\delta(x - f(t))\, m \frac{\mathrm{d}^2 w(f(t),t)}{\mathrm{d}t^2}\mathrm{d}x\,. \tag{8.25}$$

The virtual displacement w^* is expressed by (8.4). The position of the moving point can be described by a quadratic function in time:

$$f(t) = x_0 + \mathsf{v}t + \frac{1}{2}\dot{\mathsf{v}}t^2\,. \tag{8.26}$$

We take first-order polynomials as the shape functions describing the interpolation of the displacements (8.5). Here, $w_1(t)$ and $w_2(t)$ are the nodal displacements in time. This is a natural assumption since the finite element edge is straight for simple shape functions describing linear displacement distributions in the element. In such cases, the third term of (8.24) reduces to zero. That is why we must write the Renaudot formula (8.24) in a different form:

$$\begin{aligned}\frac{\mathrm{d}^2 w(f(t),t)}{\mathrm{d}t^2} = {} & \left.\frac{\partial^2 w(x,t)}{\partial t^2}\right|_{x=f(t)} + \mathsf{v}\left.\frac{\partial^2 w(x,t)}{\partial x \partial t}\right|_{x=f(t)} + \dot{\mathsf{v}}\left.\frac{\partial w(x,t)}{\partial x}\right|_{x=f(t)} + \\ & + \mathsf{v}\frac{\mathrm{d}}{\mathrm{d}t}\left[\left.\frac{\partial w(x,t)}{\partial x}\right|_{x=f(t)}\right].\end{aligned} \tag{8.27}$$

The fourth term of (8.27) is developed in a Taylor series in powers of the time increment $\Delta t = h$

$$\left[\left.\frac{\partial w(x,t)}{\partial x}\right|_{x=f(t)}\right]^{t+h} = \left[\left.\frac{\partial w(x,t)}{\partial x}\right|_{x=f(t)}\right]^{t} + \\ + \left\{\frac{\mathrm{d}}{\mathrm{d}t}\left[\left.\frac{\partial w(x,t)}{\partial x}\right|_{x=f(t)}\right]\right\}^{t}(1-\gamma)h + \left\{\frac{\mathrm{d}}{\mathrm{d}t}\left[\left.\frac{\partial w(x,t)}{\partial x}\right|_{x=f(t)}\right]\right\}^{t+h}\gamma h\,. \tag{8.28}$$

The upper indices indicate the time at which the respective terms are defined. Using (8.8), we assume the backward difference formula ($\gamma = 1$). After classical minimization of the equation (8.25) with respect to (8.27) and (8.8), we obtain

$$\mathbf{M}_m = m\begin{bmatrix} (1-\kappa)^2 & 0 & \kappa(1-\kappa) & 0 \\ 0 & 0 & 0 & 0 \\ \kappa(1-\kappa) & 0 & \kappa^2 & 0 \\ 0 & 0 & 0 & 0 \end{bmatrix}, \tag{8.29}$$

$$\mathbf{C}_m = \frac{m\mathsf{v}}{b}\begin{bmatrix} -(1-\kappa) & 0 & 1-\kappa & 0 \\ 0 & 0 & 0 & 0 \\ -\kappa & 0 & \kappa & 0 \\ 0 & 0 & 0 & 0 \end{bmatrix}, \tag{8.30}$$

$$\mathbf{K}_m = \frac{m}{b}\left(\frac{\mathsf{v}}{h}+\dot{\mathsf{v}}\right)\begin{bmatrix} -(1-\kappa) & 0 & 1-\kappa & 0 \\ 0 & 0 & 0 & 0 \\ -\kappa & 0 & \kappa & 0 \\ 0 & 0 & 0 & 0 \end{bmatrix}, \tag{8.31}$$

and

$$\mathbf{e}_m = \frac{m\mathsf{v}}{bh}\begin{bmatrix} (1-\kappa)(w_2-w_1) \\ 0 \\ \kappa(w_2-w_1) \\ 0 \end{bmatrix}, \tag{8.32}$$

with coefficient $\kappa = (x_0 + \mathsf{v}h + 1/2\,\dot{\mathsf{v}}h^2)/b\,,\ 0 < \kappa \leq 1$. κ is a parameter which defines the position of the mass in the element at the beginning of the time increment.

This determines the position of the mass at time $t = h$, related to the finite element length b. The different terms describe the transverse inertia force related to the vertical acceleration, the Coriolis force, and the centrifugal force. The matrix factors $\mathbf{M}_m$, $\mathbf{C}_m$, and $\mathbf{K}_m$ can be called the mass, damping, and stiffness matrices. The last

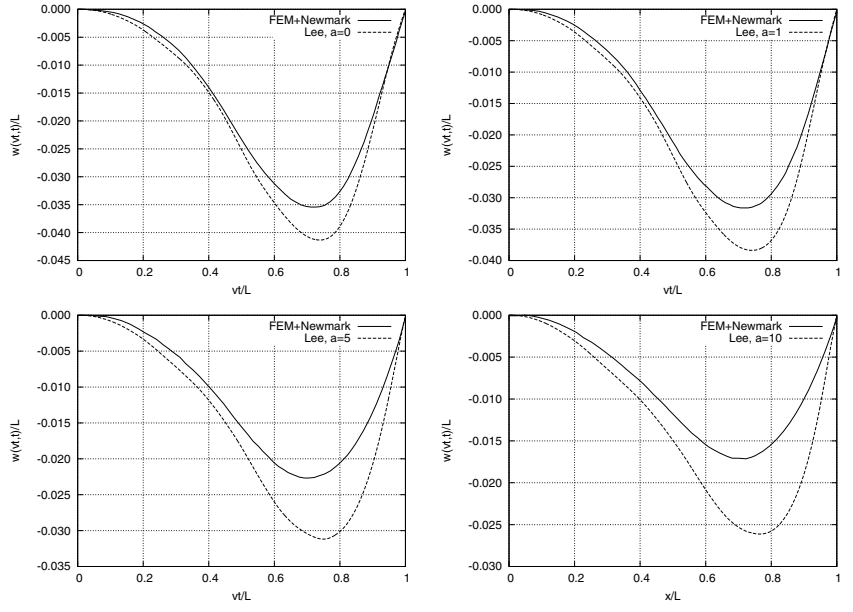

Fig. 8.11 Comparison of displacements of a Bernoulli–Euler beam under a moving contact point with those published by Lee [84]—acceleration parameter $\bar{a} = 0, 1, 5, 10$.

term $\mathbf{e}_m$ describes the nodal forces at the beginning of the time interval $[t_i, t_i + \Delta t]$. We must emphasize here that the matrices (8.29)–(8.31) and the vector (8.32) contribute only the moving inertial particle effect. The matrices of the mass influence in a finite element of a structure must be added to the global system of equations. We note that the matrices (8.29)–(8.31) differ from the matrices that result in divergence of the solution in the case of direct differentiation of (8.24)[1].

[1] Matrices that result in divergence:

$$\mathbf{M}_m = m \begin{bmatrix} (1-\kappa)^2 & 0 & \kappa(1-\kappa) & 0 \\ 0 & 0 & 0 & 0 \\ \kappa(1-\kappa) & 0 & \kappa^2 & 0 \\ 0 & 0 & 0 & 0 \end{bmatrix} \quad \mathbf{C}_m = \frac{2m\mathrm{v}}{b} \begin{bmatrix} -(1-\kappa) & 0 & 1-\kappa & 0 \\ 0 & 0 & 0 & 0 \\ -\kappa & 0 & \kappa & 0 \\ 0 & 0 & 0 & 0 \end{bmatrix},$$

$$\mathbf{K}_m = \frac{m\dot{\mathrm{v}}}{b} \begin{bmatrix} -(1-\kappa) & 0 & 1-\kappa & 0 \\ 0 & 0 & 0 & 0 \\ -\kappa & 0 & \kappa & 0 \\ 0 & 0 & 0 & 0 \end{bmatrix}, \quad \kappa = \frac{x_0 + \mathrm{v}h + \frac{1}{2}\dot{\mathrm{v}}h^2}{b}, \quad 0 < \kappa \leq 1.$$

8.6.3 Accelerating Mass—Examples

Now we will compare the displacements under a moving mass obtained from our approach with the reference results by Lee [84]. The Bernoulli–Euler beam of length $l = 6$ m, bending stiffness $EI/\rho/A = 275.4408\ \mathrm{m}^4/\mathrm{s}^2$, moving mass $m = 0.2\rho/A/l$, initial velocity at $x = 0$ of $\mathrm{v}_0 = 6$ m/s, acceleration $a = \bar{a}EI/\rho/A/l^3$ was assumed for dimensionless coefficient $\bar{a} = 0$, 1, 5, and 10 (Figure 8.11).

The Timoshenko beam was also considered in [87]. We compare our results with those published in the reference paper [86], using the same data, already listed at the beginning of this section. The acceleration $a = \mathrm{v}/\mathrm{v}_{cr}$, where the critical velocity $\mathrm{v}_{cr} = \pi/l\sqrt{EI/\rho/A}$. The acceleration $\dot{\mathrm{v}}$ is defined by a non-dimensional parameter $\kappa = \dot{\mathrm{v}}\rho Al^3/E/I$. Two cases were considered: First the case of $\beta = 0.03$, $a = 0.11$ was computed and is depicted in Figure 8.12 for the acceleration $\kappa = 1$, for a constant speed $\kappa = 0$, and for a small retardation ($\kappa = -0.05$). Figure 8.13 presents the case for a higher initial speed $a = 0.5$ and $\beta = 0.03$, for a constant speed $\kappa = 0$, and acceleration with $\kappa = 1$.

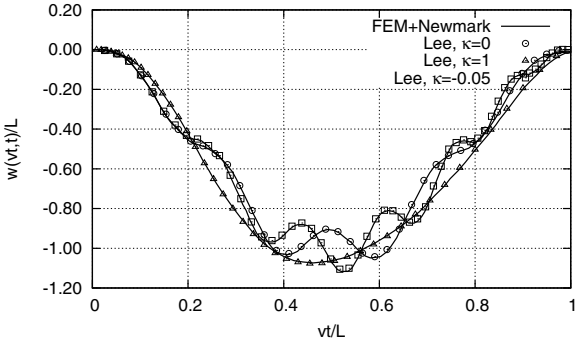

Fig. 8.12 Comparison of displacements of a Timoshenko beam under a moving contact point with those published by Lee [87]—$\beta = 0.03$, $a = 0.11$.

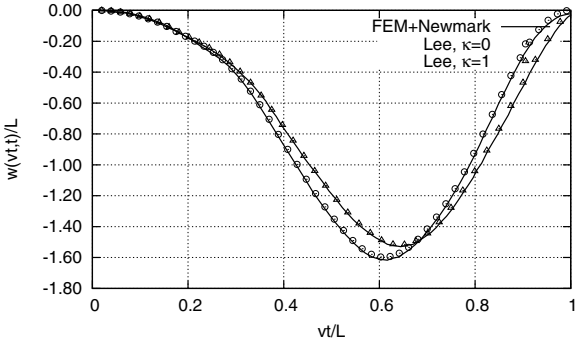

Fig. 8.13 Comparison of displacements of a Timoshenko beam under a moving contact point with those published by Lee [87]—$\beta = 0.03$, $a = 0.5$.

8.7 Conclusions

In this section we proposed a new approach to the vibration analysis of structures subjected to a moving inertial particle by use of the finite element method in space and a general time integration method, for example SSpj, in time, here represented by the Newmark and Houbolt methods. The elements describing a moving massive particle (7.29)–(7.31) can be commonly used both in the Euler beam and the Timoshenko beam. Their appearances are simpler than those of the classical matrices (8.14)–(8.16) for the Euler beam. In engineering practice, most dynamic simulations are performed by the Newmark method. An approach which extends a group of problems that can be directly solved by this commonly used method is valuable. We showed that these matrices yield accurate and stable solutions for a mass moving on a structure. Timoshenko beams or other shear resistant structures exhibit discontinuities in their solutions of the differential equations [48, 49]. Although in practice nonlinear effects smooth the trajectories, large jumps in the physical quantities are observed. The same computational result should be obtained both by semi-analytical and numerical tools. There is no reason for saying that numerical solutions converge to inaccurate results. Our finite element approach proves that even simple elemental matrices derived from a mathematically correct analysis can give perfect convergence to the analytical expressions.

There are two different ways to numerically treat differential equations in structural dynamics. The first one requires the separation of the spatial variables and time, after which two different discretizations are applied to space and to time, and finally two different solution methods are used. Commonly, the finite element method is applied to space while the central difference method or the Newmark method is applied to time. Thus the time marching procedure is established. In this case the equilibrium of forces is provided a selected time-instants, separated in time by the time step. This approach is based on a strong form of the problem. It is well elaborated for problems defined by differential equations with constant coefficients. Variable coefficients require deriving the time integration method starting from the differential equation. Classical inertia and stiffness matrices related to space can not be directly brought to play in a classical time integration method.

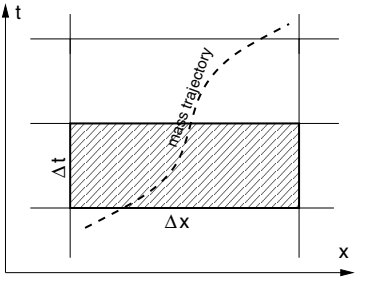

Fig. 8.14 The mass trajectory in space and time.

The second approach, called the space–time formulation [17, 9, 22], is based on the equilibrium of the energy of a structure in a time interval (Figure 8.14). It is based on the weak formulation and allows us to solve much more complicated problems, including moving concentrated physical parameters. This approach was successfully applied to the moving mass problem, solved by discrete methods [25, 24, 26].

Although the space–time approach in the case of a differential equation with constant coefficients and stationary discretization results in practically the same algorithms as the classical time integration methods, most engineers select the methods of the Newmark group for computing. A simple modification of the inertia matrix in the Newmark algorithm or direct differentiation of the acceleration of the mass particle according to the equation describing its position in time and then incorporating the resulting matrices into the solution method fails.

The practice of numerical simulations, however, requires simplicity and efficiency in the procedures. The characteristic matrices for an inertial particle should be capable of being easily incorporated into computer procedures. Thus all existing commercial codes would gain new calculating abilities. We will focus our attention on this aim.

Several classical methods for the numerical integration of the differential equations of motion can be included in one general formula, derived from the expansion of the motion function into a Taylor series. The displacements and derivatives are written in short as follows:

$$\mathbf{y}_{i+1} = \sum_{q=0}^{p-1} \frac{\Delta t^q}{q!} \mathbf{y}_i^{(q)} + \frac{\Delta t^p}{p!} \mathbf{y}_{i+\alpha}^{(p)}, \quad \dot{\mathbf{y}}_{i+1} = \sum_{q=1}^{p-1} \frac{\Delta t^{q-1}}{(q-1)!} \mathbf{y}_i^{(q)} + \frac{\Delta t^{p-1}}{(p-1)!} \mathbf{y}_{i+\alpha}^{(p)}. \quad (8.33)$$

Here, $\mathbf{y}_i$ are the known values and subsequent derivatives $\dot{\mathbf{y}}_i$, $\ddot{\mathbf{y}}_i$, etc. $\alpha_i^{(p)}$ contains unknown coefficients in terms of the remainder of the development. The above expansions allow us to write a family of methods. The general time integration method is characterized by two parameters: p, the number of terms in the Taylor series, and j, the order of the differential equation. We can construct more or less complex integration patterns, choosing the appropriate Taylor series. In the particular case $p = 2$ and $j = 2$, the method is identical with the Newmark method, and for $p = 3$ and $j = 2$, it coincides with the Houbolt method. Other well known algorithms are covered by the formula (8.33) as well. In further tests we will use the Newmark method and the Houbolt method.